# NUMERICAL SIMULATION OF A HYBRID SOLAR DRYER FOR AGRICULTURE PRODUCTS

**José Pereira Alencar Junior, jpereira@les.ufpb.br**
LES/UFPB - Universidade Federal da Paraíba

**Andrea Samara Santos de Oliveira, andrea@les.ufpb.br**
CEFET-CE, LES/UFPB - Universidade Federal da Paraíba

**Zaqueu Ernesto da Silva, zaqueu@les.ufpb.br**
LES/UFPB - Universidade Federal da Paraíba

***Abstract.*** *Conservation of long duration of fruit and vegetables preserving their food values, requires a pre-treatment of drying. Artificial drying of foodstuffs is an important method of preservation of a wide variety of products. A mathematical model based on the balance equation of heat and mass for simulating the behaviour of a solar batch dryer in forced convenction is presented. Also, we present the influence of some parameters over the behavior. A solar air flat plate collector tranfer thermal power to the drying air, and during periods of low sunshine a heater is used. The drying process was represented by a phenomenological mass tranfer model that incorporate the drying constant. Onion was chosen because of its swift deterioration property. We take account the variation of its thermal and physical properties during the drying process. The results show that drying is affected by the surface of the collector, the air temperature, the air velocity and the product characteristics.*

***Keywords****: drying, solar dryer, numerical study, drying kinetics, onion*

## 1. INTRODUCTION

Removing water from the agricultural products constitutes a significant portion of the processing activity for person working in the food and agricultural processing industries. Two major moisture removal methods are: drying to produce a solid product and evaporation to produce a more concentrated liquid. Drying and dehydration are often used interchangeably, especially when referring to food products. Drying is the most common form of food preservation and extends the food shelf life. Dehydration of foods is aimed at producing a high density product, which when adequately packaged has a long shelf life, after which the food can be rapidly and simply reconstituted without substantial loss of flavour, texture, color and aroma. Onions are generally dried from a initial moisture content of about 86% (wet basis) to 7% or less for efficient storage and processing (Kiranoudis et al., 1993). Dehydrated onions in the form of flakes or powder are in extensive demand in several parts of the world. Dehydrated onions are a product considerable importance in world trade (Sarsavadia et al., 1999).

Open sun drying is practiced widely in tropical countries. Considerable saving can be obtained with this type of drying since the source of energy is free and renewable. However, this technique is extremely weather dependent and has the problems of contamination, infestation and microbial attack. Also, the required drying time for a given commodity can be quite long. Where feasible, solar drying often provides most cost-effective drying technique, such a technique uses the energy from the sun to heat a stream of air which in turn flows by forced convection through a tray of commodity to be dried. Since the material is contained there is less contamination and it is less susceptible to adverse weather condition (Ratti and Mujumdar, 1997).

The model used by Youcef-Aly et al. (2001), to study the solar batch dryer, was based on the equation of heat applied to the product and on the equation of the drying rate. In order to represent the moisture transfer, they have used Combes model (Daguenet, 1985), which considers electrical analogies. Variation in the moisture content and influence of many parameters, such as air velocity, were studied.

In this paper, the proposed solar dryer is a simple model. A solar air flat plate collector is connected to the dryer in order to heat ambient air using free solar energy. A heater can be used during unfavorable climatic conditions. In this way, there is no need for storage system and the dryer should be practical and inexpensive for the agriculture producer.

## 2. DESIGN OF THE SYSTEM

The typical diagram of the solar batch dryer is showed in Fig. 1, this type of dryer presents some advantages like, low space requirements, easy cleaning and maintenance. The first part of the system is the drying chamber (Fig. 2) that consists of a polystyrene plate used as an insulator and a brick wall, with 0.04 m and 0.1 m thick respectively, supporting 10 trays depending of the drying condition. The space between one tray and another is 0.1 m. For a best control of the drying process, forced convection is created by a fan on the top of the dryer, in order to homogenize the air inside of drying chamber. The second part is the solar flat plate collector, used to heating the air, it consist of a glass Pyrex plate, 0.01 m thick used as a cover. An aluminum plate painted in black with 0.001m, is used as an absorber and as insulator is used a polystyrene plate 0.04 m thick. The air flow is between the absorber and insulator. The space between cover and absorber and the absorber and the insulator is 0.02 m and 0.01 m respectively. In the case of unfavorable climatic conditions, a heater is added to the dryer, it is used when the outlet temperature of the air collector is lower than a minimal temperature required, for example 333 K. So, a control system is required.

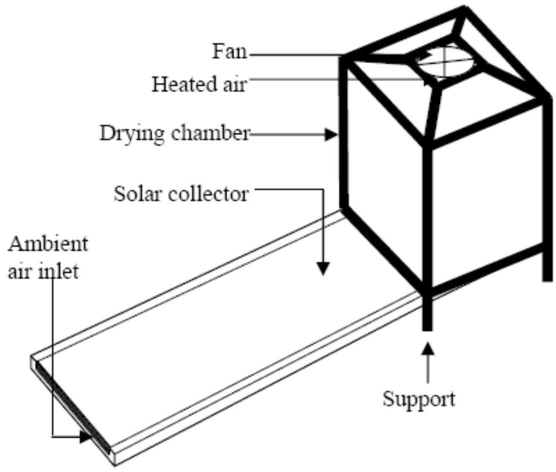


Figure 1. Diagram of a solar batch dryer

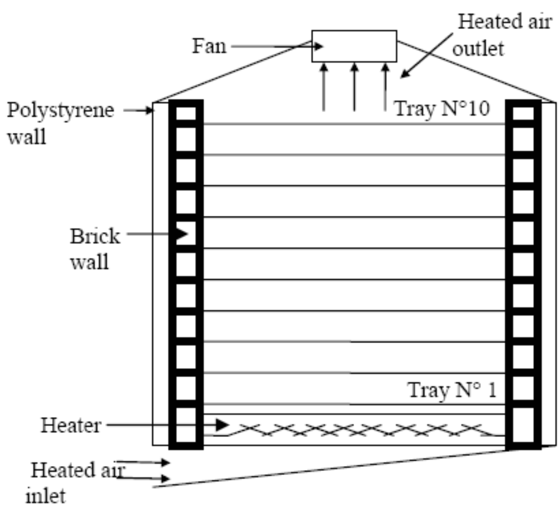


Figure 2. Internal diagram of the dryer chamber

### 3. MATHEMATICAL MODEL

One of the methods most adapted to study of this type of dryer is the "step by step method" (Daguenet, 1985). It consists of taking a fictitious slice noted "j", then generalizing the study to all system by varying "j". This method is used for both the drying chamber and the air flat plat collector.

#### 3.1. The air flat plate collector

A heat balance leads to the following equations:

At the external surface of the glass:

$$\frac{m_v C_{pv}}{A}\left(\frac{dT_{ev}}{dt}\right) = q_v" + hr_{v,céu}(T_{céu} - T_{ev}) + h_{v,amb}(T_{amb} - T_{ev}) + k_v(T_{iv} - T_{ev}) \quad (1)$$

where, $m_v$ means mass of the glass [kg], $C_{pv}$ - specific heat of the glass [J / (kg·K)], A – exchange surface [m$^2$], $\frac{dT_{ev}}{dt}$ - external temperature variation with time, $q_v$" - energy flux [W/m$^{2]}$, $hr_{v,céu}$ - adapted radiative exchange coefficient between glass and sky [W/(m$^2$·K)$^{]}$, $T_{céu}$ - sky temperature estimation [K], $T_{ev}$ - external temperature of the glass [K],

$h_{v,amb}$ - coefficient of heat transfer by convection between glass and environment [W/(m$^2$·K)], $T_{amb}$ - environment temperature [K], $k_v$ - glass conductive exchange coefficient [W/(m$^2$·K)] and $T_{iv}$ - internal temperature of the glass [K].

At the internal surface of the glass:

$$\frac{m_v C_{pv}}{A}\left(\frac{dT_{iv}}{dt}\right) = hr_{v,abs}(T_{abs} - T_{iv}) + h_{v,abs}(T_{abs} - T_{iv}) + k_v(T_{ev} - T_{iv}) \tag{2}$$

where, $\frac{dT_{iv}}{dt}$ - internal temperature variation with time [K/s], $hr_{v,abs}$ - adapted radiative exchange coefficient between glass and insulator [W/(m$^2$·K)], $T_{abs}$ - insulator temperature [K] and $h_{v,asb}$ - coefficient of heat transfer by convection between glass and insulator[W/(m$^2$·K)].

At the absorber plate:

$$\frac{m_{abs} C_{pabs}}{A}\left(\frac{dT_{abs}}{dt}\right) = h_{v,abs}(T_{iv} - T_{abs}) + hr_{v,abs}(T_{iv} - T_{abs}) + hr_{abs,iso}(T_{i,iso} - T_{abs}) + h_{fld,abs}(T^{old} - T_{abs}) + q_{abs}'' \tag{3}$$

where, $m_{abs}$ means mass of the absorber [kg], $C_{pabs}$ - specific heat of the absorber [J / (kg·K)], $\frac{dT_{abs}}{dt}$ - absorber temperature variation with time [K/s], $q_{abs}$" - energy flux [W/m$^2$], $hr_{v,abs}$ - adapted radiative exchange coefficient between glass and absorber [W/(m$^2$·K)], $hr_{abs,iso}$ - adapted radiative exchange coefficient between absorber and insulator [W/(m$^2$·K)] , $h_{fld,abs}$ - coefficient of heat transfer by convection between air and absorber [W/(m$^2$·K)] , $T^{old}$ - air temperature at precedent time [K] and $T_{i,iso}$ - internal temperature of the insulator [K].

At the air flows:

$$\dot{m}_{ar} C_{par}\left(T - T^*\right) = A h_{fld,abs}(T_{abs} - T^*) + A h_{fld,i,iso}(T_{i,iso} - T^*) \tag{4}$$

where, $\dot{m}_{ar}$ means air mass flow rate [kg/s], $C_{par}$ - specific heat of the air [J / (kg·K)], T - air temperature [K] and $h_{fld,iso}$ - coefficient of heat transfer by convection between air and insulator [W/(m$^2$·K)].

At the internal surface of the insulator:

$$\frac{m_{iso} C_{piso}}{A}\left(\frac{dT_{i,iso}}{dt}\right) = hr_{abs,iso}(T_{abs} - T_{i,iso}) + h_{fld,i,iso}(T^{old} - T_{i,iso}) + k_{iso}(T_{e,iso} - T_{i,iso}) \tag{5}$$

where, $m_{iso}$ means mass of the insulator [kg], $C_{piso}$ - specific heat of the insulator [J/kg·K], $\frac{dT_{i,iso}}{dt}$ - internal insulator temperature variation with time [K/s], $hr_{abs,iso}$ - adapted radiative exchange coefficient between absorber and insulator [W/(m$^2$·K)], $k_{iso}$ - insulator conductive exchange coefficient [W/(m$^2$·K)] and $T_{e,iso}$ - external temperature of the insulator [K].

At the external surface of the insulator:

$$\frac{m_{iso} C_{piso}}{A}\left(\frac{dT_{e,iso}}{dt}\right) = k_{iso}(T_{i,iso} - T_{e,iso}) + hr_{s,iso}(T_s - T_{e,iso}) + h_{iso,amb}(T_{amb} - T_{e,iso}) \tag{6}$$

where, $\frac{dT_{e,iso}}{dt}$ - external insulator temperature variation with time [K/s], $hr_{s,iso}$ - adapted radiative exchange coefficient between ground and insulator [W/(m$^2$·K)], $T_s$ - ground temperature [K] and $h_{iso,amb}$ - coefficient of heat transfer by convection between insulator and environment [W/(m$^2$·K)].

* represents the precedent tray.

The terms $q_v''$ and $q_{abs}''$ depend on the direct and the diffuse received energy flux. On addition, they depend on the direct and diffuse absorptivity of the material.

### 3.2. The drying chamber

The heat and mass balance allows the establishment of the following equations:

At the flow of the heated air:

$$\dot{m}_{arq} C_{par} \left( T_{arq}^{*} - T_{arq} \right) = h_{arq,c} A_c (T_{arq} - T_c) + 4 h_{arq,i,par} A_{par} (T_{arq} - T_{i,par}) \tag{7}$$

where, $\dot{m}_{arq}$ means heated air mass flow rate [kg/s], $T_{arq}$ – heated air temperature [K], $h_{arq,c}$ - coefficient of heat transfer by convection between heated air and onion [W/(m$^2$·K)], $A_c$ – exchange surface of the onion [m$^2$], $h_{arq,i,par}$ - coefficient of heat transfer by convection between heated air and internal walls of the dryer [W/(m$^2$·K)] and $T_{i,par}$ – internal walls temperature [K].

At the product:

$$m_c C_{pc} \left( \frac{dT_c}{dt} \right) = h_{arq,c} A_c (T_{arq} - T_c) - q_{eva}'' \tag{8}$$

where, $m_c$ means mass of the onion [kg], $C_{pc}$ - specific heat of the onion [J / (kg·K)], $\frac{dT_c}{dt}$ - onion temperature variation with time [K/s] and $q_{eva}$” – evaporative power [W/m$^2$].

At the internal surface of the brick wall:

$$\frac{m_{pt} C_{pt}}{4} \left( \frac{dT_{i,par}}{dt} \right) = k_t A_{par} (T_{poli} - T_{i,p}) + h_{arq,i,p} A_{par} (T_{arq} - T_{i,p}) \tag{9}$$

where, $m_{pt}$ means mass of the brick wall [kg], $C_{pt}$ - specific heat of the brick wall [J / (kg·K)], $\frac{dT_{i,par}}{dt}$ - brick wall internal temperature variation with time [K/s] , $k_t$ – brick wall conductive exchange coefficient [W/(m$^2$·K)], $T_{poli}$ – polystyrene wall temperature [K], $T_{i,p}$ – internal temperature of the brick wall [K], $h_{arq,i,par}$ - coefficient of heat transfer by convection between heated air and the brick wall [W/m$^2$K], $q_{eva}$” – evaporative power [W/m$^2$].

Between the brick and the polystyrene walls:

$$\frac{m_{ppoli} C_{ppoli}}{4} \left( \frac{dT_{poli}}{dt} \right) + k_{poli} A_{poli} (T_{poli} - T_{e,p}) = \frac{m_{pt} C_{pt}}{4} \left( \frac{dT_{poli}}{dt} \right) + k_t A_{poli} (T_{poli} - T_{i,p}) \tag{10}$$

where, $m_{ppoli}$ means mass of the polystyrene wall [kg], $C_{ppoli}$ - specific heat of the polystyrene wall [J / (kg·K)], $\frac{dT_{poli}}{dt}$ - polystyrene wall temperature variation with time [K/s] , $k_{poli}$ – polystyrene wall conductive exchange coefficient [W/(m$^2$·K)] and $T_{e,p}$ – external temperature of the polystyrene wall [K].

At the external surface of the polystyrene wall:

$$\frac{m_{ppoli} C_{ppoli}}{4} \left( \frac{dT_{e,par}}{dt} \right) = k_{poli} A_{par} (T_{poli} - T_{e,p}) + h_{amb,e,p} A_{par} (T_{amb} - T_{e,p}) + hr A_{par} (T_{céu} - T_{e,p}) \tag{11}$$

where, $\frac{dT_{e,par}}{dt}$ - brick wall external temperature variation with time [K/s], $h_{amb,e,p}$ - coefficient of heat transfer by convection between ambient air and the external polystyrene wall [W/m$^2$K],. hr - coefficient of heat transfer by radiation between external polystyrene wall and sky [W/m$^2$K].

* represents the precedent tray.

The term $q_{eva}''$ is the evaporative power:

$$q_{eva}'' = m_{\sec} L_{eva} \frac{dX}{dt} \tag{12}$$

where, $m_{sec}$ is dry product mass [kg], $L_{eva}$ – latent heat of vaporization [J/kg] and dX/dt – moisture content variation with time [kg / (kg dry basis · s)].

$A_c$ may be evaluated by:

$$A_c = \pi D^2 n \tag{13}$$

where, n is the number of products put on each tray and D – diameter of the product.

Kiranoudis et al. (1993) proposed calculate the variation of air humidity using the following expression:

$$(W_{arq,0} - W_{arq})\dot{m}_{arq} = K_f (X - X_e) m_{\sec} \tag{14}$$

where, $W_{arq}$ is the heated air absolute humidity [kg/kg], $W_{arq,0}$ – precedent heated air absolute humidity [kg/kg], $K_f$ – the drying constant, X – product moisture content [kg / kg dry basis] and $X_e$ – equilibrium moisture content of dehydrated product [kg / kg dry basis].

The variation of X, which represents the moisture content of the product during the drying time, is needed.

### 3.2. Drying Kinetics

Mathematical models are necessary for the analysis and design of a drying process. The complexity of the appropriate model depends on the purpose of the application considered. Detailed models are needed for dynamics simulations and control, while simplified models are needed for design or state estimation techniques. In this study we use a phenomenological mass transfer model, this one can be formulated by assuming that the rate of moisture loss, dX/dt is proportional to the instantaneous difference between material moisture content, X, and the expected material moisture content when it comes into equilibrium with the drying air, Xe (Kiranoudis et al., 1992).

$$-\frac{dX}{dt} = K_f (X - X_e) \tag{15}$$

The drying constant ($K_f$) depends on the product characteristic dimension "D", air temperature "$T_{arq}$", humidity "$W_{arq}$" and velocity "$U_{arq}$". Then, each type of product has its own $K_f$ for a specific experimental condition and it can be calculated as follows:

$$K_f = \beta_0 D^{\beta_1} T_{arq}^{\beta_2} W_{arq}^{\beta_3} U_{arq}^{\beta_4} \tag{16}$$

where, $\beta_0$, $\beta_1$, $\beta_2$, $\beta_3$ e $\beta_4$ are empirical coefficients which can be estimated by fitting the total model used to the experimental drying curves (Kiranoudis et al., 1992) .

The equilibrium moisture content of materials can be described by several mathematical models with two or more parameters. The more number of parameters the more complicate is the model and harder to analyze and use it. Kiranoudis et al. (1993) estimates GAB equation parameters for onion and other vegetables, which includes parameters with physical meaning:

$$X_e = \frac{X_m C k a_w}{(1 - k a_w)(1 - (1 - C) k a_w)} \tag{17}$$

In this expression, $X_e$ is the equilibrium moisture content, $a_w$ is the water activity, $X_m$ is the monolayer moisture content, while C and k are related to the temperature.

In this work, the onion is approximated by a spherical body, which has 87.6% of relative moisture in the beginning of the process and its composition is: 87.60% of water, 1.25% of proteins, 4.91% of carbohydrates, 0.25% of fat and 5.99% others.

Singh (1996) said that specific heat of the onion could be evaluated by:

$$C_{pc} = 1{,}424 m_{carboidratos} + 1{,}549 m_{proteínas} + 1{,}675 m_{gordura} + 0{,}837 m_{outros} + 4{,}187_{água} \tag{18}$$

The physical characteristics are recalculated for each time step and for each batch of the dryer, which allows the shrinking effects to be taken into account (Bennamoun & Belhamri, 2003). Its necessary to calculate the heated air velocity around the product ($U_{arq}$):

$$U_{arq} = U / Po \tag{19}$$

where, U is the air velocity inside the drying chamber and Po – porosity rate:

$$Po = 1 - Oc \tag{20}$$

where, Oc is the occupation rate:

$$Oc = n\frac{\pi D^3}{6}\frac{1}{Comp \cdot L\arg \cdot D} \tag{21}$$

where, Comp and Larg are the length and the width of the batch dryer respectively.

### 3.2. Resolution method

The solution of both sets of equations are found using programs developed in FORTRAN language, the first one concerning the air flat collector and the other the drying chamber. The IMSL subroutine is used to resolve the two sets of equations written in matrix form.

There are two approaches to the system:

Case 1 (without heater): when the heated air temperature is equal to the outlet air collector;

Case 2 (with heater): when the outlet air collector temperature is less than 333 K then the heated air temperature is equal to 333 K (heater turned on). Otherwise, the heated air temperature is equal to the outlet air collector.

## 4. RESULTS AND DISCUSSION

In the processes of indirect solar drying, the flat plate collector is connected to the drying chamber. Knowing that when the air flow rate increases, for the same radiation received by the flat plate collector, the air temperature at the exit of this one decreases. The drying time is fixed in 10 hours for all simulation. We therefore will study the influence of the climatic parameters of the drying air on the behavior of the product during drying and will try to find a compromise between velocity and temperature. The solar radiation data used in simulation was from $16^{th}$ of January 2007 given by the IMEP station in the LES/UFPB, as shows the Tab. 1, in this region the sunrise at 6:00 a.m. We decide to start the drying process at 7 a.m., due to the inertia of the system with low level of solar irradiation (Bennamoun and Belhamri, 2003). Initially, the solar batch dryer without heater is studied. The influence of the heater during unfavorable climatic conditions is analyzed later.

Table 1. Values of hourly global solar irradiation in $16^{th}$ January 2008 at João Pessoa.

| | | | | | | | |
|---|---|---|---|---|---|---|---|
| Time of the day (h) | 6 | 7 | 8 | 9 | 10 | 11 | 12 |
| Radiação (kJ/m²) | 43.43 | 642.9 | 1583 | 2218 | 2809 | 3620 | 3765 |
| Time of the day (h) | 13 | 14 | 15 | 16 | 17 | 18 | |
| Radiação (kJ/m²) | 3689 | 3162 | 2554 | 1883 | 774.6 | 44.11 | |

The influence of the collector surface on the outlet air temperature is show in the Fig. 3. In this figure the energy received in the first 20 minutes is used to warm-up the collector. After this time the heated air temperature raises and is directly related to the absorbed energy and the ambient temperature. Their increasing implies its increase and their decrease leads to its decrease. The absorbed energy, which is at this time transmitted to the air, increases with the increase of the collector surface. Therefore, the outlet air temperature from de collector increase by increasing the collector area surface. It is important to note that the maximum temperature is achieved between noon and 1 p.m.

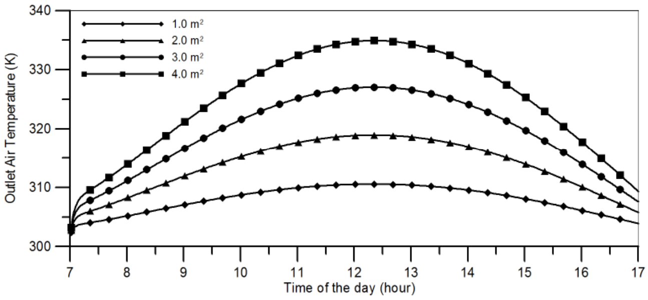


Figure 3. Influence of the solar collector surface on its outlet air temperature.
(Tamb = 302.0 K, RHamb = 70%, Air Flow Rate = 0.15 $m^3/s$, Air Channel Depth = 0.020 m)

The influence of the collector surface on the product moisture content without a heater is showed in Fig 4. In the beginning of drying an insignificant decrease of the moisture content is registered. After 60 minutes the heat is transmitted to the air and thus to the product. So, there is a noted diminution in the product moisture content with the surface increasing. Moreover, at 4 $m^2$ the product moisture had reached the purposed moisture content after 600 minutes. The purposed moisture content varies from 0.111 to 0.136 kg/kg d.b. In this range, the characteristics like odour, flavour, texture, colour and the nutritional amount remain unaltered. For the $1m^2$ collectors surface the moisture content reached after 10 h is inadequate to storage.

Figure 5 represents the influence of the collector surface on the product temperature, in the dryer without a heater at the $10^{th}$ tray. Due to the ambient temperature and relativity humidity from the region, the behavior of product temperature is similar to the air heating in the solar collector.

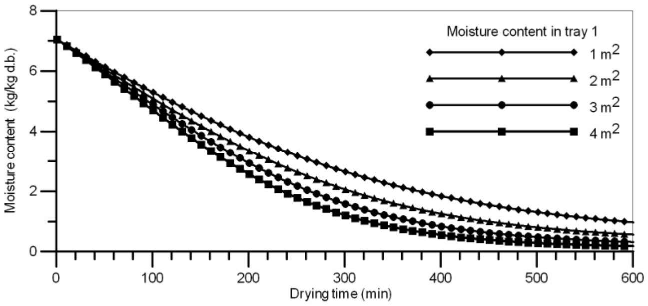


Figure 4. Influence of the solar collector surface on the product moisture content
(Tamb = 302.0 K, RHamb = 70%, Air Flow Rate = 0.15 $m^3$/s, Air Channel Depth = 0.020 m)

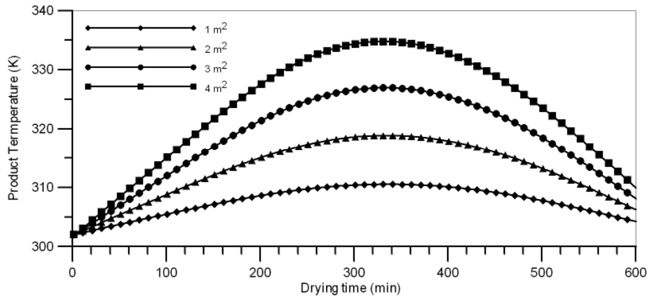


Figure 5. Influence of the collector surface on the product temperature.
(Tamb = 302.0 K, RHamb = 70%, Air Flow Rate = 0.15 $m^3$/s, Air Channel Depth = 0.020 m)

The importance of adding a heater to all solar collector surfaces is shows in Fig. 6. The uses of a heater is very important, the Fig. 3 has showed that the heated air temperature had exceeded 333 ºC only for a 4 $m^2$ collector surface only between 12 and 13 h. Under these conditions, after total drying time, the product has not attained the proposed moisture content. The uses of a heater allow drying the product in unfavourable conditions, mainly in the beginnings 300 min of drying. However, for a dryer with a heater, the product is dried with constants 333 ºC. The difference between theses moisture contents can be clearly observed in the Fig. 6. Consequently, after adding a heater, the purposed moisture content was achieved after 600 min of drying.

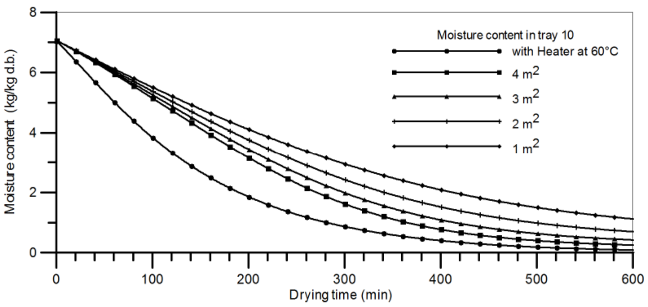


Figure 6. Influence of the collector surface on the product moisture content.

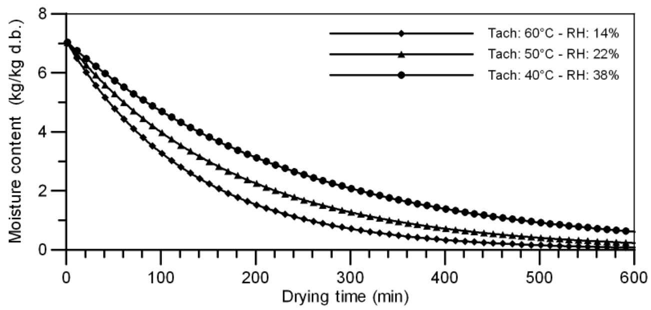


Figure 7. Influence air drying temperature on the evolution of the product reduced moisture content

Figure 7 shows the influence of the heated air temperature on the product moisture content in the first rack where the process proceeds at constant temperature, the air flow rate is fixed at 1.0 $m^3$/s and its air temperature varying for 313, 323 and 333 K, for an ambient air temperature 302 K with a relative humidity 70%.

The curves highlight the influence of the air temperature at the entry of the drier on the evolution of the product reduced moisture content according to time. They show the moisture content is very sensitive to the variation of the drying temperature. The final moisture content is very small when the temperature is higher, which is explained by the growth of the drying rate (Youcef-Ali et al, 2001).

The Fig. 8 shows the influence of the air velocity at the entry of the drier, on the evolution of the reduced moisture content of the onion located on the first and last rack, according to time. In this case the air temperature is fixed at 333 K, for the three air flux rates, and the relative humidity is fixed at 14 %. For the same air temperature, the influence of the increase of the air flux rate, which favours the heat and mass exchange, is weaker than that of the temperature, we can note in the last trays (n = 10) the influence is so strong than in the first trays, but in the end of drying is so quite of the first trays. The drying time is weaker when we increase the air flow rate.

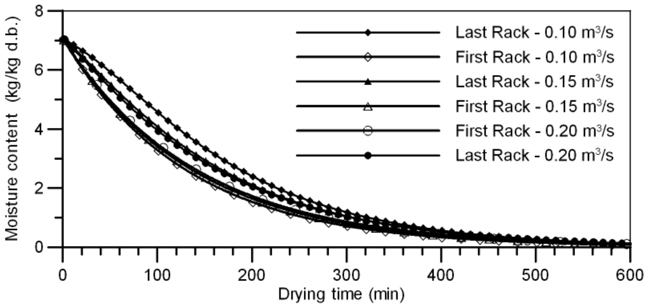


Figure 8. Influence of the air flux rate on the evolution of the onion reduced moisture content.

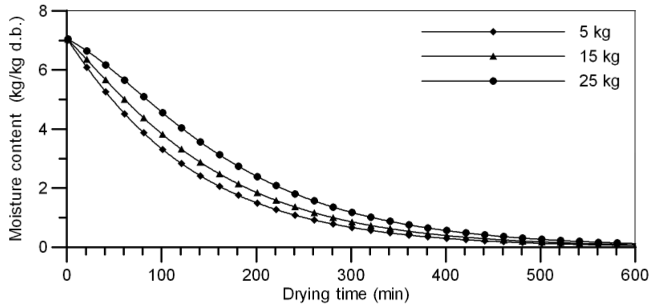


Figure 9. Influence of the product mass on the evolution of the product moisture content

We note that for these two cases, which proceed under the same conditions of the temperature and relative humidity, the product have been dried after 600 minutes (10 h). Now we represent in Fig. 9 the influence of the product mass on the moisture content at the $10^{th}$ tray. When the heated air crosses the product, the water evaporated until reached the equilibrium moisture. As the product is a hygroscopic one, the equilibrium moisture is different from zero. Note that that the moisture content of 25 kg is more important than 5 kg, because the drying time is near of 600 min. So, increasing the mass implies increasing the number of onion put on each tray of the dryer.

## 5. CONCLUSION

We have established a mathematical model of numerical simulation, which allows the study of the performances of a foodstuffs drier with racks. The mains parameters that affect the solar batch drying are the collector surface and the temperature of the heated air. Their changes affects considerably the drying time, so their increase reduces the drying time. Using heated allows to drying at constant temperature during all drying process and under unfavorable climatic conditions.

Using a solar batch dryer with 4 $m^2$ and a heated air at 333 K allows use a dryer chamber with 10 tray with capacity of 25 kg each one, per day.

The study can be developed for some other agriculture products to predict the behaviour of the solar batch dryer, in different seasons.

## 6. REFERENCES


Bennamoun, Lyes and Belhamri, A. 2003, “Design and Simulation of a Solar Dryer For Agriculture Products”, Journal of Food Engineering, 59, pp. 259-266.

Kiranoudis, C.T., Maroulis, Z.B., Tsami, E., J., & Marinos-Kouris, D. 1993. “Equilibrium Moisture Content and Heat of Desorption of Some Vegetables”. Journal of Food Engineering, 20, 55-74.

Kiranoudis, C.T., Dimitratos, J., Maroulis, Z.B., & Marinos-Kouris, D. 1993. “State estimation in the batch drying of foods”. Drying Tecnology, 11, (5), 1053-1069.

Kiranoudis, C.T., Dimitratos, J., Maroulis, Z.B., & Marinos-Kouris, D. 1992. “Model selection in air drying of foods”.. Drying Tecnology, 10, (4), 1097-1192.

Kiranoudis, C.T., Maroulis, Z.B., Dimitratos, J., Marinos-Kouris, D. 1992. “Drying kinetics of onion and green pepper”. Drying Tecnology, 10, (4), 995-1011.

Kiranoudis, C.T., Maroulis, Z.B., Tsami, E., J., & Marinos-Kouris, D. 1993. “Equilibrium Moisture Content and Heat of Desorption of Some Vegetables”. Journal of Food Engineering, 20, 55-74.

M. Daguenet, “Les Séchoirs Solaires: theorie at pratique”, UNESCO, France, 1985.

Ratti, C., Mujumdar, A. S., 1997, “Solar Drying of Foods: Modeling and Numerical Simulation”, Solar Energy Vol. 60, No. 3/4, pp. 151-157.

S. Youcef-Ali, J. Y. Desmons, A. Abene, H. Messaoudi and M. Le Ray., 2001.“Numerical and Experimental Study of the Drying of a Potato in Forced Convection in a Drier with Racks”,

Sarsavadia, P.N., Sawhney, R.L. , Pangavhane, D.R., Singh, S.P. 1999. “Drying behavior of brined onion slices”. Journal of Food Engineering, Vol. 40, pp. 219-226

Singh, R.P. 1996. “Food Engineering”. In R.C. Dorf (Ed.), The Engineering Handbook, p. 1786, Florida, CRC Press Handbook.


## 7. RESPONSIBILITY NOTICE

The author(s) is (are) the only responsible for the printed material included in this paper.